BIORHEOLOGY, 28; 401-419, 1991
0006-355X/91 $3.00 + .00 Printed in the USA.


# THE SPECIFIC HYDRAULIC CONDUCTIVITY OF BOVINE SERUM ALBUMIN

Annabelle Kim, ChunHai Wang, Mark Johnson and Roger Kamm
Massachusetts Institute of Technology,
Cambridge, MA, USA

(Received 8.3.1991; accepted in revised form 17.7.1991 by Editor T. Laurent)

## ABSTRACT

Previous studies of extracellular matrix hydraulic conductivity have characterized the flow resistance of glycosaminoglycans, proteoglycans and collagen. This work focusses on serum albumin, present in significant quantities in many connective tissues, but not previously considered for its role in determining connective tissue flow resistance. The specific hydraulic conductivity of bovine serum albumin solutions, as a function of concentration, was calculated from sedimentation and ultrafiltration data available in the literature. A rigid particle hydrodynamic model compared favorably with these results.

Experimental measurements on an albumin ultrafiltration cell were in agreement with this model (within experimental error); furthermore, the experimental data confirmed the theoretical prediction that there is no (or negligible) pressure drop through the concentration polarization layer. Use of the hydrodynamic model for albumin specific hydraulic conductivity with literature values for the hindrance of albumin when passing through a glycosaminoglycan (GAG) matrix allows an estimate of the relative importance of the albumin on tissue hydraulic conductivity: in non-cartilagineous tissues with moderate GAG concentrations, tissue levels of albumin can generate flow resistance effects comparable to those of the GAGs, although well less than the flow resistance of these tissues.

## INTRODUCTION

The flow resistances of a variety of physiologic tissues have been characterized by the hydraulic conductivity of solutions of its individual macromolecular constituents. Previous studies have focused on the glycosaminoglycans (GAGs), in particular hyaluronic acid. Day (1) found that the action of hyaluronidase significantly increased tissue hydraulic conductivity, prompting the hypothesis that hyaluronic acid was the source of tissue resistance. However, Jackson and James (2) showed that the specific hydraulic conductivity[1] of hyaluronic acid (in fact, all GAGs) failed to account for the

KEY WORDS: Extracellular matrix (ECM), bovine serum albumin (BSA), hydraulic conductivity, glycosaminoglycan (GAG)

[1] By specific hydraulic conductivity (3), we refer to K in Darcy's law defined as $K=\mu QL/(\Delta PA)$ where $\mu$ is the fluid viscosity, $Q$ the flow rate , $L$ the length of the porous medium, $\Delta P$ the pressure drop across the porous medium and $A$ the cross-sectional area facing flow.

high flow resistance of the extracellular matrix[2] (ECM). Levick (3) has shown that this conclusion is valid for a wide variety of tissues, although recent evidence suggests (4) that GAGs may well account for the bulk of flow resistance of cartilagineous tissues. Many researchers (2,3,5-7) have suggested that proteins may contribute to the resistance of the ECM tissues. Ethier et al. (7), for example, found that inclusion of the GAG-associated proteins in calculations of specific hydraulic conductivity for the corneal stroma greatly improved agreement with measured values.

Plasma proteins are a constituent of the extracellular matrix that are not normally considered with regard to extracellular matrix hydraulic conductivity. Albumin is the predominant plasma protein, the primary contributor to the colloid osmotic pressure (which in part governs the exchange between the vascular system and the ECM) and is ubiquitous in connective tissues. 60% of the body's albumin is found in the extravascular space (8): the approximate extravascular albumin concentration in human skin is 6.5–12 mg/gram tissue (9), in human muscle is 2.7-6.4 mg/gram tissue (9), in peripheral rabbit cornea is 6-9 mg/gram tissue (20% of plasma) (10) and in the rabbit ciliary processes is 22-33 mg/gram tissue (74% of plasma) (11). Consequently, it is of interest to examine the effect of albumin on the specific hydraulic conductivity of the ECM.

Bovine serum albumin (BSA) is a well-characterized protein with relevant properties (molecular weight, partial specific volume, friction factors, etc.) (12) that are similar to those of human albumin. In the current study, the specific hydraulic conductivity of BSA, as a function of concentration, is determined based on information available in the literature; a semi-empirical model is developed. Experimental confirmation of this model is obtained using a ultrafiltration cell that is also used to examine the pressure distribution within the albumin layer accumulated at the surface of the rejecting membrane (the concentration polarization layer). The semi-empirical model for albumin specific hydraulic conductivity is combined with data on the specific hydraulic conductivity of hyaluronic acid to predict what effects albumin might have on connective tissue flow resistance. We find that while connective tissue levels of albumin can generate flow resistance effects comparable to those of the glycosaminoglycans, this resistance is not sufficient to explain the flow resistance of these tissues.

## METHODS

### Specific Hydraulic Conductivity Determination

The specific hydraulic conductivity of macromolecular solutions may be calculated from sedimentation data using the relation (13):

$$K = \frac{\mu_1 s}{c_2(1 - v_2 \rho_1)} \qquad [1]$$

where $\mu_1$ is the viscosity of the solvent in which the macromolecule is sedimenting, $s$ the sedimentation coefficient, $c_2$ the concentration of the macromolecule, $v_2$, the partial specific volume of the

[2] by ECM, we mean the macromolecular complex surrounding the cells, including collagen, elastin, proteoglycans, GAGs, structural glycoproteins and plasma proteins.

macromolecule (for BSA, 0.734 ml/g (12)), and $\rho_1$ the density of the solvent.[3]

A second approach is to model the macromolecular solution as a porous medium and calculate specific hydraulic conductivity from ultrafiltration data using Darcy's Law:

$$\frac{dP}{dx} = -\frac{\mu_1 Q}{K A} \qquad [2]$$

where $dP/dx$ is the pressure gradient in the porous medium, $Q$ the volume flow rate, and $A$ the cross-sectional area perpendicular to the flow. ($Q/A$ is the superficial velocity of the fluid relative to the macromolecules.) For macromolecular systems, it has been shown (14) that a modified form of Darcy's law should be used:

$$\frac{d(P - \Pi)}{dx} = -\frac{\mu_1 Q}{K A} \qquad [3]$$

This may be viewed as a force balance on the solvent in which the pressure and osmotic forces driving the fluid into the concentration polarized layer are balanced by the viscous drag forces. This relationship has been derived thermodynamically considering the gradient in solvent chemical potential while applying the Gibbs-Duhem condition and Onsager reciprocity (15).

Three differing derivations (14,16,17) have shown that in a concentration polarization layer, provided that gelation does not occur, the pressure gradient, $dP/dx$, is zero. Thus equation [3] becomes:

$$\frac{d\Pi}{dx} = \frac{\mu_1 Q}{K A} \qquad [4]$$

(This result can also be derived by considering a mass balance for solute in the concentration polarization layer using the Stokes-Einstein relationship for diffusivity (18).)

Expressing $\Pi$ as a function of protein concentration, equation [4] can be written as:

$$\frac{d\Pi}{dc_2}\frac{dc_2}{dx} = \frac{\mu_1 Q}{K A} \qquad [5]$$

Thus, if the dependence of $\Pi$ on $c_2$ is known and the concentration gradient in the concentration polarization layer is measured, the specific hydraulic conductivity can be determined as a function of concentration (for known values of Q and A).

Ultrafiltration Cell

A schematic of the ultrafiltration system is given in Figure 1 (18). The system involves a constant pressure supply (provided by a $CO_2$ tank and regulator), pressure sensor, ultrafiltration cell with adjustable needle probe, and filtrate collection bottle. The pressure regulator controlled the upstream pressure to $\pm$ 20 mm Hg. The flow chamber has an inner diameter of is 2.2 cm and a length of 2.8 cm.

[3]In what follows, the subscript 1 refers to the saline solvent, 2 to albumin and 3, where appropriate, to a hyaluronate matrix.

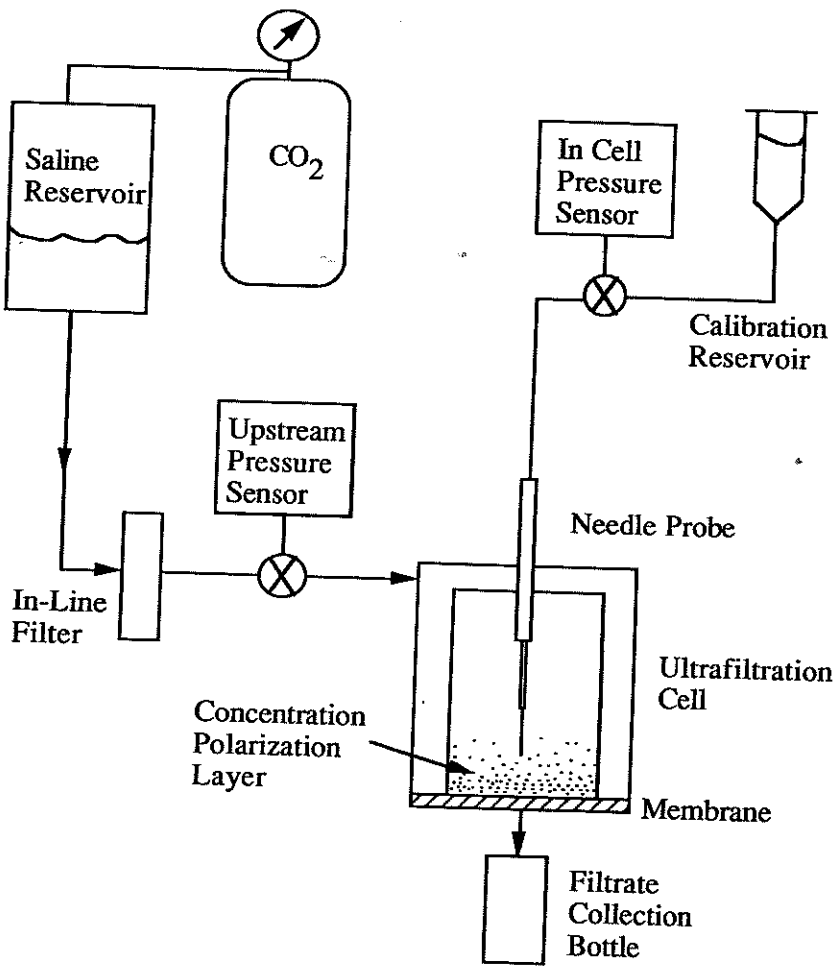


Figure 1: Schematic of ultrafiltration system.

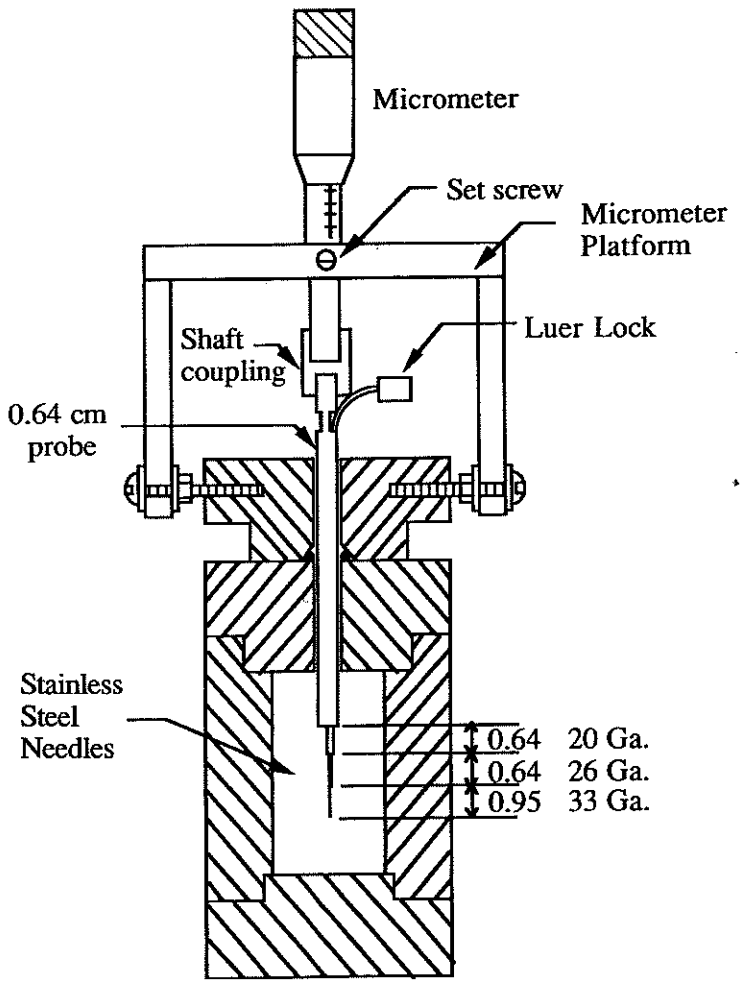


Figure 2: Ultrafiltration cell – Micrometer-Driven Needle Probe Assembly (dimensions in centimeters; not to scale).

The ultrafiltration cell (plexiglass) and pressure needle probe (stainless steel) are shown in Figure 2. The needle probe and micrometer assembly is fixed to the ultrafiltration cell by three set screw in the collar of the micrometer platform. The micrometer (Mitutoyo Model 153-204, Harbor Control, Westwood, MA) has a 0-25 mm range with 0.001 mm graduations. The non-rotating micrometer spindle is connected to a 0.64 cm diameter stainless steel tube by a 0.64 cm coupling that has been bored out at one end to fit the 0.8 cm diameter micrometer spindle. The stainless steel tube is approximately 7.6 cm in length and has a side hole through which has been passed a 20-ga (0.09 cm OD) stainless steel tube with Luer lock. The needle is epoxied into place, and the end of the larger tube is sealed with epoxy. A length of 26-ga (0.046 cm OD) stainless steel tubing is epoxied into the 20-ga needle. A length of 33-ga (0.02 cm OD) stainless steel tubing is epoxied into the 26-ga needle; it is this latter tube that is used to measure the pressure within the concentration polarization layer. The fluid-filled pressure probe is connected to the pressure sensor by sterile pressure tubing.

At the bottom of the ultrafiltration cell is the ultrafiltration membrane (PTGC 02510, Millipore, Bedford, MA), supported by a porous polypropylene frit, which was used to reject the albumin. Its nominal molecular weight cut-off is 10 kilodaltons. Membrane flow resistance was measured in all experiments, using pure solvent filtration, and found to be several orders of magnitude smaller than the total resistance of the BSA layer in all cases reported. Accounting for gaskets, the membrane surface area was 3.4 $cm^2$.

The albumin solution used in the perfusion studies was made using BSA (BSA fraction V, Boehringer Mannheim Biochemicals, Indianapolis, IN), buffered saline (Dulbecco's phosphate buffered saline, pH = 7.3, Life Science Technologies, Chagrin Falls, OH) and sodium azide (0.02%) (Fluka, Ronkonkoma, NY) added to prevent bacterial growth. Solvent and solutions were sterilized by filtering with a 0.2 μm Gelman Acrodisc filter. In order to coat the binding sites on the inner surface of the ultrafiltration cell, the cell was soaked overnight in filtered 0.05 g/ml BSA solution. In one set of experiments, fluoresceinated BSA (No. A-9771, Sigma, St. Louis, MO.) was used to allow visualization of the concentration polarization layer.

The BSA solution (approximately 5 ml) was added carefully to the bottom of the ultrafiltration cell and then covered with buffered saline. This was done in an effort to reduce the time frame required for the concentration polarization layer to form. Care was taken to eliminate any bubbles from the system. Filtration experiments were conducted for about one month; this extended period was due to the time required for the concentration polarization layer to reach an equilibrium state. The filtration pressure was monitored by the upstream pressure sensor (model #136PC100G2, Microswitch, Newton, MA).

Filtrate was collected in a collection bottle connected via tubing to the ultrafiltration cell; a mineral oil layer covered this filtrate fluid reservoir to prevent evaporation. This collection bottle was periodically weighed on an electronic scale (Sartorius model 1419, Westbury, NY) to determine the filtration rate. Flowrate measurements were taken over time periods of 350 hours and were accurate to approximately $5x10^{-3}$ μl/min. Flowrates ranged between 0.1 and 1 μL/min.

After a steady-state condition was reached (determined by monitoring filtrate flowrate as a function of time), the pressure distribution in the cell was measured by the needle probe connected to a pressure transducer (model #136PC100G2, Microswitch, Newton, MA). Pressures were measured

throughout the concentration polarization layer, every 0.1 cm well away from the membrane, every 0.01 cm as the membrane was approached. Distance from the ultrafiltration membrane was determined by advancing the micrometer until the needle probe penetrated the membrane (at the conclusion of the measurement process) and then determining all distances relative to this distance.

For use in the data analysis, osmotic pressure measurements were carried out independently on solutions made from the same materials. An ultrafiltration membrane (PTGC 01310, Millipore, Bedford, MA) was placed into a Millipore filtration cell (SX0001300, Millipore, Bedford, MA). The filtration cell was attached directly to a pressure transducer (model #136PC100G2, Microswitch, Newton, MA) and the cell filled with the albumin solution. Tubing and connections were kept short to minimize system compliance. On the opposite side of the membrane was buffer in a column. The pressure increase in the cell was then monitored as a function of time until osmotic equilibration was achieved. The measurement was conducted at room temperature. The volume change due to system compliance was a negligible fraction of cell volume such that dilution effects were insignificant.

## RESULTS

### Specific Hydraulic Conductivity Determination

Sedimentation and ultrafiltration data available in the literature were used to calculate the specific hydraulic conductivity of BSA. Sedimentation coefficients for BSA (12,19-23) were used in equation [1] to calculate specific hydraulic conductivity with the result plotted in Figure 3. Despite the range of solvent, pH and ionic strength conditions, the specific hydraulic conductivities are well-described by a single curve.

Vilker (24) conducted ultrafiltration studies on BSA and measured the concentration profile in the concentration polarization layer at various flowrates. In separate experiments, Vilker (25) also obtained osmotic pressure data under the same solvent, pH and membrane reflection coefficient conditions as his ultrafiltration experiments. These data were used with equation [5] to determine the specific hydraulic conductivity. The results are plotted along with the sedimentation results on Figure 3. There is general agreement between the two methods of determining specific hydraulic conductivity although the Vilker data appear to deviate from the general behavior for concentrations ~ 0.1 g/ml.

### Modelling the Specific Hydraulic Conductivity of BSA

The balance of pressure drop and viscous drag for particles moving through solvent (as in sedimentation) or experiencing a solvent flux (as in ultrafiltration) yields, in the dilute limit,

$$K = \frac{\mu_1}{n_2 f} \qquad [6]$$

where $n_2$ is the number of particles per unit volume and f is the frictional coefficient per spherical particle. The frictional coefficient for the non-spherical BSA molecule is given by the Perrin factor $f/f_0 = 1.147$ (19) with $f_0$, the frictional coefficient for an equivalent isolated sphere, given by:

$$f_0 = 6\,\pi\,\mu_1\left[\frac{3\,m_2\,v_2}{4\,\pi}\right]^{1/3} \qquad [7]$$

where $m_2$ is the mass of a BSA molecule . Substituting [7] into [6] and using a BSA molecular weight of 67,000 (19) and solvent viscosity of water (0.01 poise) yields the theoretical relationship for specific hydraulic conductivity at dilute concentrations:

$$K = 1.90 \times 10^{-14}\, c_2^{-1} \qquad [8]$$

where K is in units of $cm^2$ and $c_2$, BSA concentration, is in $g/cm^3$. In the limit of low concentration ( $c_2 < 0.01$ g/ml), a least square fit of the BSA specific hydraulic conductivity data shown in figure 3 yields:

$$K = 1.60 \times 10^{-14}\, c_2^{-1.008} \qquad [9]$$

with r = 0.992 (correlation coefficient) and n =7 (number of data points). The expected concentration dependence is observed within a reasonable error.

At higher concentrations, the specific hydraulic conductivity is more strongly dependent on concentration. Albumin is a globular protein, usually described as a prolate ellipsoid with reported values of axial ratio ranging from 3–3.5 (19,25). We used correlations for the sedimentation of concentrated solutions of rigid spheres to examine the hypothesis that albumin behaves hydrodynamically like a rigid particle. The most commonly used empirical correlation for the hindered settling function of rigid spheres is attributed to Richardson and Zaki (1954):

$$h\,(\Phi_{\text{sphere}}) = \left[1 - \Phi_{\text{sphere}}\right]^{5.1} \qquad [10]$$

where $h\,(\Phi_{sphere})$ is the ratio of hindered settling velocity to Stokes settling velocity, and $\Phi_{sphere}$ is the sphere volume fraction (26). Introducing this relation into equation [1] yields:

$$K = \frac{\mu_1\, s_0\, h\,(\Phi_{\text{sphere}})}{c_2\left(1 - v_2\,\rho_1\right)} \qquad [11]$$

where $s_0$, the sedimentation coefficient at infinite dilution, is determined by the low concentration specific hydraulic conductivity data (using equations [1] and [9]); this semi-empirical approach also includes the Perrin factor (thus accounting for ellipticity and hydration) .

The solid sphere volume fraction, $\Phi_{\text{sphere}}$, is equivalent to the volume fraction of BSA including any bound or associated solvent which would move with the sedimenting protein. This quantity was calculated from the hydrated molecular volume ($V_m$) as:

$$\Phi_{\text{sphere}} = c_2\,\frac{N_a\,V_m}{M_2} \qquad [12]$$

where $V_m = 1.5 \times 10^{-19}$ $cm^3$ (25), $N_a$ is Avogadro's number, and $M_2$ is the molecular weight of

BSA. Substituting $s_0$, $h(\Phi_{sphere})$ and $\Phi_{sphere}$ into equation [11] yields:

$$K = 1.6 \times 10^{-14} c_2^{-1} ( 1 - 1.348 c_2 )^{5.1} \qquad [13]$$

This correlation is plotted (solid line) in Figure 3. In spite of the fact that we have introduced only one adjustable parameter (the frictional coefficient at infinite dilution), the correlation agrees with the experimental data, showing a deviation from a 1/c dependence of specific hydraulic conductivity at a concentration of approximately 0.05 g/ml and passing close to the apparent mean of the available data for higher concentrations (there is increased scatter in the data for these higher concentrations).

Pressure distribution in concentration polarization layer

Our experiments on ultrafiltration of albumin solutions allowed us, using the needle probe, to make measurements of the pressure distribution within the concentration polarization layer. Figure 4 shows the distribution of pressure in this layer for two experiments with differing total amounts of albumin in the system ($m$); the total applied pressure drop was similar in the two experiments (520 and 450 mm Hg). The data shows negligible changes in pressure throughout the concentration polarization layer with the entire pressure drop occurring within in a very short distance of the membrane (0.01 cm or less). Recall here that the flow resistance of the membrane was negligible in comparison with that of the concentration polarization layer.

To ensure that our pressure measurements were made within the concentration polarization layer, fluoresceinated albumin was used in one experiment. Figure 5 shows the concentration polarization layer with the needle probe clearly within this layer. The pressure distribution for this experiment is shown in Figure 4 (m = 0.4 g).

Comparison of Predicted to Measured Flowrate

The ultrafiltration experiments also allowed us to further examine the validity of equations [4] and [13]. If we rearrange equation [5], multiply it by $c_2$, and integrate over the domain ($x=0$ to $x=\infty$; $c=c_m$ to $c=0$) we can find that:

$$Q = \frac{A^2}{\mu_1 m} \int_0^{c_m} K(c_2) \frac{d\Pi}{dc_2} c_2 \, dc_2 \qquad [14]$$

where $m$ is the total mass of solute (albumin) placed in the system and $c_m$ is the albumin concentration at the filter face. This expression can be written as:

$$Q = \frac{A^2}{\mu_1 m} \left[ \Pi(c_m) K(c_m) c_m - \int_0^{c_m} \Pi(c_2) \frac{d[K(c_2) c_2]}{dc_2} dc_2 \right] \qquad [15]$$

The concentration of albumin at the membrane ($c_m$) is determined by the condition that the entire system pressure drop occurs osmotically at the filter face and thus $\Pi_m = \Delta P$, allowing a determination of $c_m$ if the osmotic pressure dependence on concentration is known. If we now substitute equation [13] into equation [15] and use the experimental data for $\Pi(c_2)$, then for a given $\Delta P$, $m$, $A$ and $\mu_1$, we can predict the flowrate Q. Figure 6 shows our measurements for osmotic pressure as a function

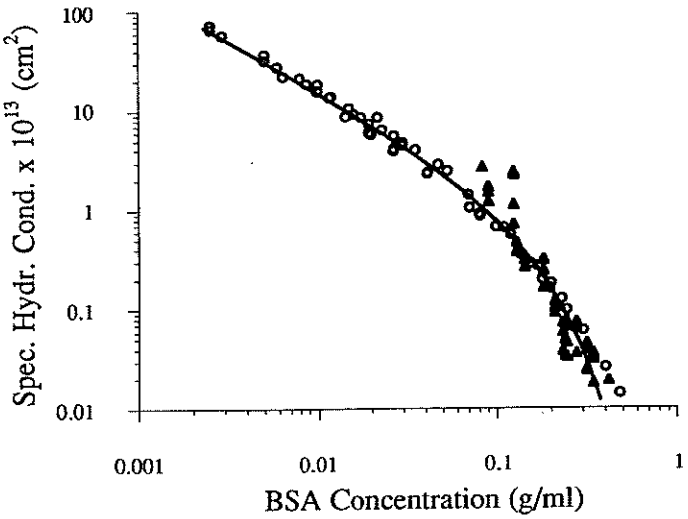


Figure 3: Specific hydraulic conductivity of bovine serum albumin as a function of concentration. The open symbols are from sedimentation studies (Squire pH 4.6 and 8.15 (19); Baldwin pH 4.55 (20); Loeb pH 4.00 and 5.13 (12); Kitchen (21); Comper pH 7 (23) and van den Berg pH 7.4 (22)) and closed symbols from perfusion studies (Vilker et al., pH 4.5,5.4 and 7.4 (24)) using equation [5]. The solid line is the semi-empirical correlation, equation [13].

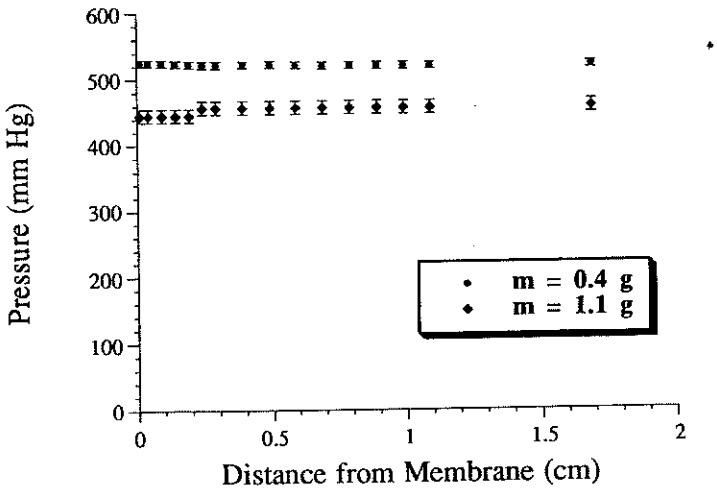


Figure 4: Pressure distribution within the concentration polarization layer measured at the conclusion of the experiment (zero pressure is downstream of the rejecting membrane). Error bars reflect uncertainty in measured pressure. Concentration polarization layer for m=0.4 g is shown in figure 5.

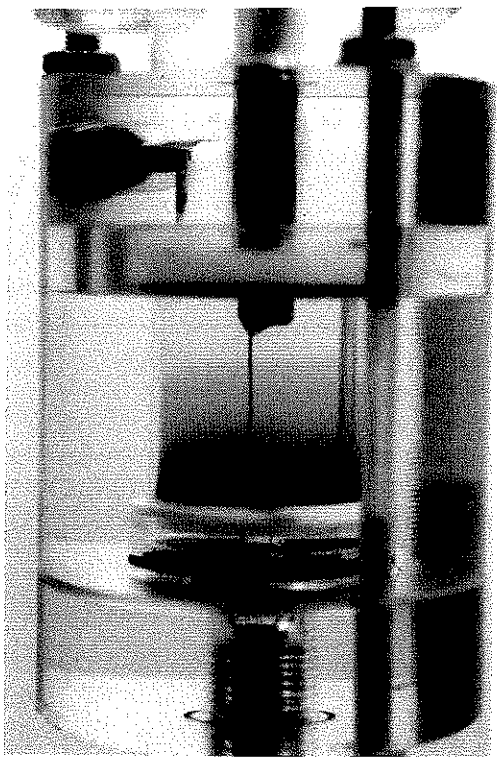

Figure 5: Photograph of fluoresceinated albumin concentration polarization layer showing the needle probe within this layer.

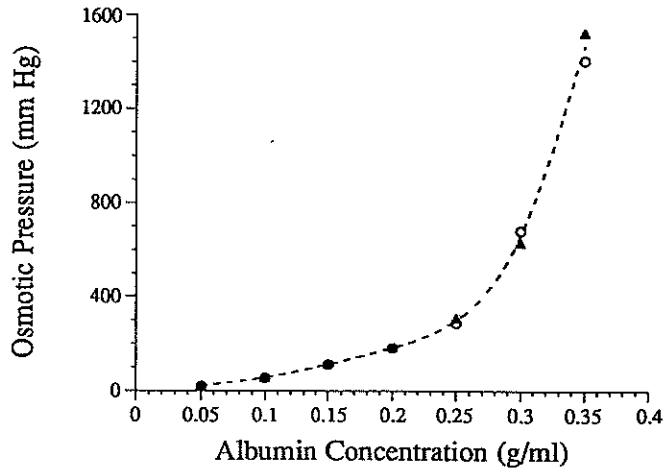


Figure 6: Osmotic pressure of albumin as a function of concentration (pH = 7.4). The two symbols are for two separate measurements. The dashed line is a spline fit to the data that was used in equation [15] to predict flowrate for the experimental perfusions.

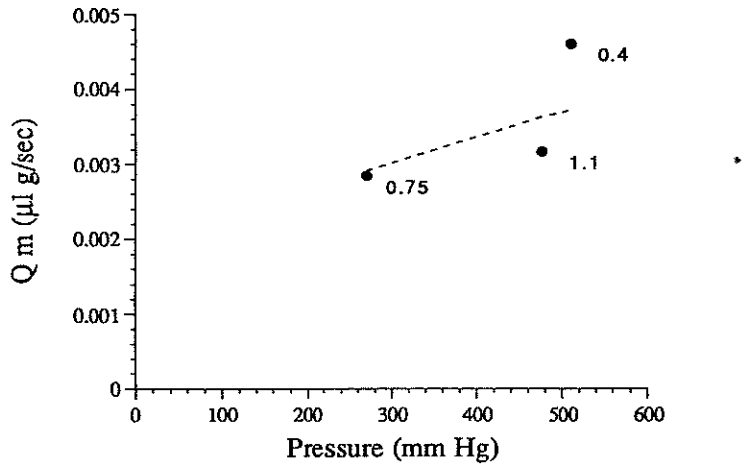


Figure 7: Flowrate times mass as a function of pressure drop across the system. The dashed line is the prediction from equation [15] while the data points are experimental measurements. The values next to the data points are the mass in grams of albumin in the ultrafiltration cell for that experiment.

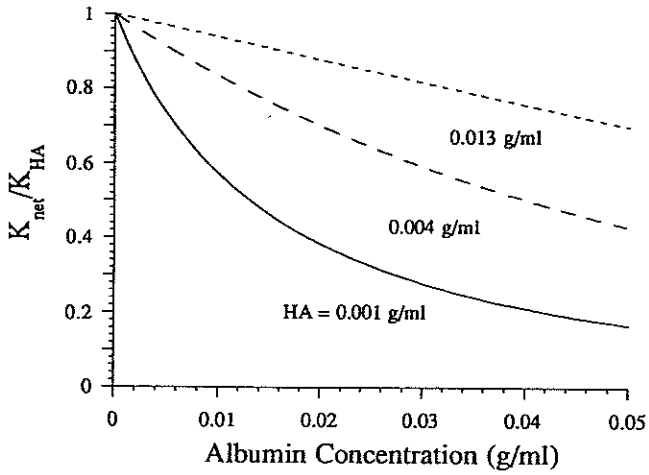


Figure 8: The ratio of the net specific hydraulic conductivity ($K_{net}$) of a mixture of hyaluronic acid and albumin, to that of hyaluronic acid alone ($K_{HA}$), for three concentrations of hyaluronic acid.

of albumin concentration and a best fit of these data (these data fall between those of references (23) and (25)). Using these data in conjunction with equations [13] & [15] allows us to predict the flow rate for any given $\Delta P$.

Equation [15] indicates that $Q\,m$ should be a unique function of $\Delta P$ (in so far as $\Delta P$ establishes $c_m$). Figure 7 shows a plot of the experimental results versus the theoretical predictions. The pressures reported here are averaged over the time period of the flow measurement. Given the experimental uncertainties (flowrate, regulated pressure variations, osmotic pressure determination, albumin concentration at filter face), the results are in reasonable agreement with the predictions. (Note that, as opposed to Figure 3, the ordinate in this figure is arithmetic, not logarithmic).

## DISCUSSION

In this study, we have determined the specific hydraulic conductivity of albumin solutions as a function of concentration using data from sedimentation studies and from direct perfusion studies. The values for specific hydraulic conductivity, as determined by equations [1] (sedimentation experiments) and [5] (concentration polarization experiments), were found to be in reasonable agreement with one another, as shown in Figure 3. Along with a determination of the specific hydraulic conductivity of albumin over a wide range of concentrations, this approach also confirmed the experimental validity of equations [4],[5]. Interestingly, the data did not show the specific hydraulic conductivity to depend on solution pH.

A semi-empirical model was developed to characterize the dependence of specific hydraulic conductivity on albumin concentration. Modelling albumin as a hydrated sphere (in spite of its ellipsoidal character), and using an experimental correlation for the specific hydraulic conductivity of a solution of spheres, we obtained an expression in agreement with the experimental data on the specific hydraulic conductivity of bovine serum albumin, showing both good agreement with the qualitative character of the data and reasonable quantitative agreement allowing for experimental scatter. The physiological range of tissue albumin concentration (based on the values reported above and typical tissue extracellular hydration) is roughly 0.01–0.2 g/ml.

Experiments were conducted to further validate this model. Albumin was placed into an ultrafiltration cell and perfused with buffer. Figure 5 shows the concentration polarization layer near the membrane surface. In this layer, the solute molecules adjust themselves such that their convection toward the membrane is exactly balanced by their diffusion away from the membrane. If we assume the diffusion coefficient of albumin to be roughly constant and we define the thickness of the concentration polarization layer as the distance from the membrane at which the albumin drops to 1% of its value that it had at the membrane surface (x=0), then we can characterize the thickness of the albumin layer as $5D/V$ where $D$ is the diffusion coefficient of the albumin and $V$ the velocity of solvent passing through the system. For our experiments, this thickness is predicted to be approximately 1 cm, consistent with the results from use of the fluorescent probe. (Actually, of course the probe can be seen throughout the cell, but most of the fluorescence occurs within 1 cm of the membrane surface).

We determined the hydrostatic pressure distribution within this concentration polarization layer. The concentration polarization layers investigated were such that the distribution of albumin in the cell was far from the average concentration that would be expected in the absence of flow. These average concentration (0.04–0.1 g/ml) would generate osmotic pressures of 10-60 mm Hg; as the system pressure drop was 500 mm Hg, substantial concentration polarization occurred with the albumin concentration nearest the membrane of approximately 0.3 g/ml ($c_m$) (see figure 6) .

Our experiments established (Figure 4) that the pressure gradient in this layer is indeed zero (or negligible), as predicted theoretically (14,16,17). Note that this result does not imply that there is negligible dissipation in the concentration polarization layer: the dissipation results in a loss in chemical potential of the solvent and a resulting $d\Pi/dx$ (equation [4]). There will, of course, be a region of steep gradient in hydrostatic pressure near the membrane where the albumin is reflected by the membrane; in this region, $dP/dx=d\Pi/dx$. As our pressure measurement probe could be positioned within an accuracy of 0.01 cm, we can conclude that this pressure gradient must occur within 0.01 cm of the rejecting membrane or across the membrane itself. This result is expected to be valid for macromolecular systems that do not support a solid stress (non-gelled systems) (15). We are currently conducting experiments to determine how this result might be modified in gelled macromolecular layers.

Our experimental studies also allowed us to explore the use of the semi-empirical model to predict the hydrodynamic resistance of an albumin concentration polarization layer. Within expected experimental uncertainties, the model predictions agreed with experimental results. It should be noted here that although the system flow resistance will be determined by losses throughout the concentration polarization layer, the specific hydraulic conductivity of the high concentration of albumin nearest the membrane will dominate this resistance. We estimate (based on osmotic pressure measurements) that this concentration is approximately 0.3 g/ml, and thus the data reported here add further support to the higher concentration regime modeled by equation [13].

Application of the results to flow through connective tissues

One motivation for this study was to determine whether the albumin found within connective tissues might contribute to tissue flow resistance. For this purpose, we modelled the extracellular matrix as a fixed matrix of hyaluronic acid containing albumin that is mobile. As saline flows through this system, it carries with it the albumin, albeit at a lower velocity than the saline vehicle since the albumin is hindered in its transit by the hyaluronate matrix.

In this model, the specific hydraulic conductivity of the system is determined by the combined drag of the saline passing over the (fixed) hyaluronic acid molecules and the saline moving relative to the hindered albumin. To find the degree to which the albumin is hindered in its motion, we require data on the motion of albumin through a hyaluronic acid matrix. Laurent et al. (27,28) conducted experiments in which they determined the sedimentation and diffusion coefficient of albumin (and other macromolecules) while in solutions of hyaluronic acid. Their data can be used to find the velocity of the albumin ($V_2$), relative to its saline vehicle ($V_1$), as it is passed through a hyaluronic acid matrix (component 3):

$$\frac{V_2}{V_1} \equiv 1 - g(\Phi_3) = 1.03\, e^{-8.23*\sqrt{\Phi_3}} \qquad [15]$$

assuming the density of hyaluronic acid to be 1.85 g/ml (29), where $g(\Phi_3)$ represents the hindrance of the albumin relative to the saline vehicle due to the presence of hyaluronic acid and $\Phi_3$ the volume fraction of hyaluronic acid (this relationship has been verified for $\Phi_3<0.014$ (30)).

To calculate the drag, we followed the approach of Silberberg (15) who considered gradients in the chemical potential of a three-component system where solvent 1 contained a diffusible solute 2 which could pass through the gel phase 3 but at a velocity different than that of the solvent. The total drag force was assumed to be the sum of the drag on the gel matrix (hyaluronate) and the drag on the solute (albumin) (this is equivalent to assuming a dilute limit). The drag on the hyaluronate was determined using the interstitial velocity of the saline while that of the albumin by its velocity relative to the saline vehicle. Silberberg determined the hydraulic conductivity and rejection coefficient of such a system. His rejection coefficient $\sigma$ can be shown to be related to the hindrance function $g(\Phi_3)$ by the expression:

$$\sigma = \frac{\Phi_1\, g(\Phi_3)}{\Phi_1 + \Phi_2\,(1 - g(\Phi_3))} \qquad [16]$$

In the absence of gradients of activity of the gel or solute (homogeneous distribution) and using the hyaluronic acid matrix as the fixed reference frame, Silberberg's expression for hydraulic conductivity of the system can be used to show that:

$$\frac{1}{K_{net}} = \frac{1}{K_3} + \frac{g(\Phi_3)}{K_2} \qquad [17]$$

where $K_3$ is the specific hydraulic conductivity of the hyaluronate matrix to solvent flux, and $K_2$ is the specific hydraulic conductivity of albumin to solvent flux.

We now assume that $K_3 = K_3(\Phi_3)$ and $K_2 = K_2(\Phi_2)$. This is a simplification of the physics involved, but is correct in the limit of dilute solutions and should allow us to make a rough estimate of the effect of albumin on ECM specific hydraulic conductivity.[4] Equation [13] is used to characterize $K_2(\Phi_2)$ ; $K_3(\Phi_3)$ is determined using experimental data (6). The results of these calculations are plotted in Figure 8. An effect not included in this model is the excluded volume interaction (partition function) between albumin and ECM constituents such as collagen and hyaluronic acid (8). These interactions will increase the heterogeneity of the albumin and GAG distribution, thereby increasing the specific hydraulic conductivity (31).

The results show that in connective tissues with moderate GAG concentrations, tissue levels of albumin, while passing through the ECM, can have effects on specific hydraulic conductivity comparable to those of the GAGs. It must be recalled, however, that in non-cartilagineous connective tissues, the flow resistance generated by GAGs are generally an order-of-magnitude lower than that exhibited by the connective tissue (2,3,6,7). Thus, the model suggests that the levels of albumin and glycosaminoglycans found in the non-cartilagineous connective tissues are insufficient to explain the generation of flow resistance in these tissues; other extracellular moieties (glycoproteins, core proteins and collagen) must contribute to the generation of non-cartilagineous connective tissue flow resistance.

---

[4] Strictly speaking, these results are limited to concentrations of albumin such that the effects of albumin on hydraulic conductivity are less than those of the hyaluronic acid; otherwise the specific hydraulic conductivity of hyaluronic acid, which due to its rod-like nature is highly boundary condition dependent, would depend on the concentration of albumin in the solution.

## ACKNOWLEDGEMENTS

We acknowledgement support from the National Eye Institute (EY05503) and the National Institute on Aging (AG08289).

## REFERENCES


1. DAY,T.D. The permeability of interstitial connective tissue and the nature of the interfibrillary substance, *J. Physiol.*, 117:1-8 (1952).

2. JACKSON,G.W. and JAMES,D.F. The hydrodynamic resistance of hyaluronic acid and its contribution to tissue permeability, *Biorheology* , 19:317-330 (1982).

3. LEVICK,J.R. Flow through interstitium and other fibrous matricies, *Quarterly Journal of Experimental Physiology 72:* 409-38 (1987).

4. ZAMPARO,O. and COMPER,W.D. Hydraulic conductivity of chondroitin sulfate proteoglycan solutions, *Archives of Biochemistry and Biophysics 274:* 259-269 (1989).

5. CURRY,F.E. Is the transport of hydrophilic substances across the capillary wall determined by a network of fibrous molecules?, *Physiologist* , 23:90-93 (1980).

6. ETHIER,C.R. The hydrodynamic resistance of hyaluronic acid: estimates from sedimentation studies, *Biorheology* , 23:99-113 (1986).

7. ETHIER,C.R., KAMM,R.D., PALASZEWSKI,B.A., JOHNSON,M. and RICHARDSON,T.M. Calculations of flow resistance in the juxtacanalicular meshwork, *Invest. Ophthal. and Vis. Sci.*, 27:1741 (1986).

8. BERT,J.L. and PEARCE, R.H.The interstitium and microvascular exchange, Chapter 12 in **The Handbook of Physiology**, section 2: **The Cardiovascular System**, volume IV. Microcirculation, Part 1, volume eds. E.M. Renkin and C.C. Michel, exec. ed. S.R. Geiger, American Physiological Society, Bethesda, Maryland (1984).

9. KATZ,J., BONORRIS,G. and SELLERS,A.L. Extravascular albumin in human tissues, *Clinical Science 39*: 725-729 (1970).

10. MAURICE,D.M. and WATSON,P.F. The distribution and movement of serum albumin in the cornea, *Experimental Eye Research 4*: 355-363 (1965).

11. BILL,A. A method to determine osmotically effective albumin and gammaglobulin concentrations in tissue fluids, its application to the uvea and a note on the effects of capillary "leaks" on tissue fluid dynamics, *Acta Physiol. Scand. 73*: 511-522 (1968).

12. LOEB,G.I. and SCHERAGA,H.A. Hydrodynamic and thermodynamic properties of bovine serum albumin at low pH, *J. of Phys. Chem.*, 60:1633 (1956).

26. DAVIS,R.H. and ACRIVOS,A. Sedimentation of noncolloidal particles at low Reynolds numbers, *Ann. Rev. Fluid Mech.*, 17:91 (1985).

27. LAURENT,T.C. and PIETRUSZKIEWICZ,A. The effect of hyaluronic acid on the sedimentation rate of other substances, *Biochemica et Biophysica Acta 49:* 258-264 (1961).

28. LAURENT,T.C.,BJORK,I.,PIETRUSZKIEWICZ,A. and PERRSON,H. On the interaction between polysaccharides and other macromolecules. II. The transport of globular particles through hyaluronic acid solutions, *Biochemica et Biophysica Acta 78:* 351-359 (1963).

29. COMPER,W.D. and ZAMPARO,O. Hydrodynamic properties of connective-tissue polysaccharides, *Biochem. J.* 269: 561-4 (1990).

30. WINLOVE,C.P. and PARKER,K.H. Diffusion of macromolecules in hyaluronate gels. I. Development of methods and preliminary results, *Biorheology* 21: 347-62 (1984).

31. HAPPEL,J. and BRENNER,H. **Low Reynolds Number Hydrodynamics**, p. 372, first paperback edition, Martinus Nijhoff Publishers, the Hague, the Netherlands (1983).